

AUTOMATED LEAF-LEVEL HYPERSPECTRAL IMAGING OF SOYBEAN PLANTS USING AN UAV WITH A 6 DOF ROBOTIC ARM

by
Jialei Wang

A Thesis

Submitted to the Faculty of Purdue University

In Partial Fulfillment of the Requirements for the degree of

Master of Science in Mechanical Engineering



School of Mechanical Engineering

West Lafayette, Indiana

August 2021

THE PURDUE UNIVERSITY GRADUATE SCHOOL
STATEMENT OF COMMITTEE APPROVAL

Dr. Xiulin Ruan, Co-chair

School of Mechanical Engineering

Dr. Jian Jin, Co-chair

School of Agriculture and Biological Engineering

Dr. R. P. Kingsly Ambrose

School of Agriculture and Biological Engineering

Approved by:

Dr. Nicole L. Key

ACKNOWLEDGMENTS

First and foremost, I would like to express my gratitude for my advisor, Dr. Jian Jin, for his guidance. For the past five years, Dr. Jin has helped me every step of the way in both research and preparation for a professional career after graduation. I appreciate all the opportunities he has given me to work on things I am passionate about. Dr. Jin also taught me effective communication with colleagues and sponsors which are invaluable lessons for my future. I would also like to thank Dr. Xiulin Ruan and Dr. Kingsly Ambrose for taking the time to serve on my committee.

I also want to show my appreciation to all the students and postdoctoral researchers in Dr. Jin's lab. Yikai Li and Ziling Chen helped me plant and collect data on the soybeans. They also gave me many suggestions on my project which allowed me to avoid common mistakes. I have worked with Dr. Liangju Wang for many years and during this time, he has supported me on several projects and taught me many technical concepts. I would like to thank Meng-Yang Lin from Dr. Mitchel Tuinstra lab for his help with growing the soybean plants we used. Without his knowledge and expertise, the ground truth data would not be as good. Lastly, I would like to thank my friends and family for providing their support, encouragement, and wisdom.

TABLE OF CONTENTS

TABLE OF CONTENTS.....	4
LIST OF TABLES.....	6
LIST OF FIGURES	7
ABSTRACT.....	8
1. INTRODUCTION	9
1.1 Literature Review.....	10
1.1.1 Current Hyperspectral Imaging System in Agriculture	10
1.1.2 Leaf-level HSI System.....	12
1.1.3 Hyperspectral Image Modeling	14
1.2 Automatic Soybean Leaf-level Hyperspectral UAV	15
2. LEAFSPEC FOR DICOT LEAVES	16
2.1 Overview	16
2.2 Hardware Design	17
2.2.1 Hyperspectral Camera	17
Diffraction Grating and Filter	17
Lenses and Slit	18
Imaging Sensor.....	19
2.2.2 Lightbox.....	19
2.2.3 Scanning Mechanism.....	20
2.2.4 Device Open/Close Mechanism	21
2.2.5 Attachment to Robotic Arm.....	22
2.2.6 Electronics	23
Power Supply	24
MicroProcessor.....	24
MicroController.....	25
2.3 Device Operation and Data Flow.....	25
3. HS IMAGES MODELING USING LEAF NDVI DISTRIBUTION	27
3.1 Overview.....	27
3.2 Data collection	28

3.2.1	Experiment Setup.....	28
3.2.2	HS images Collection	28
3.2.3	Ground Truth Data Collection	28
3.3	Modeling Steps	29
3.3.1	Pre-processing and Modeling Setup	29
3.3.2	Modeling using Mean NDVI.....	30
3.3.3	Modeling using Leaf NDVI Heatmap	30
3.4	Modeling Result.....	31
3.4.1	Mean NDVI Modeling Result	31
3.4.2	NDVI Heatmap Distribution Model Result	32
4.	UAV FOR IN-FIELD LEAF-LEVEL HYPERSPECTRAL IMAGE COLLECTION.....	34
4.1	Overview.....	34
4.2	Current Progress.....	34
4.3	UAV Configuration	36
4.3.1	Motor and Power	38
4.3.2	Airframe.....	38
4.3.3	Flight Controller	38
4.3.4	Communication.....	39
4.3.5	Ground Station.....	39
5.	CONCLUSION AND FUTURE WORKS	41
5.1	Conclusion	41
5.2	Future Works	41
5.2.1	LeafSpec for Soybean Leaf	41
5.2.2	HS images Modeling using Leaf Distribution	42
5.2.3	In-Field UAV for Leaf-Level HS images Collection	42
	REFERENCE.....	43

LIST OF TABLES

Table 2.1 Full specification of the imaging sensor (BFLY-U3-05S2M-CS) from Teledyne FLIR	19
Table 4.1 List of parts on the UAV with the corresponding weight.....	37
Table 4.2 List of parts for the ground station.....	37

LIST OF FIGURES

Figure 1.1 A visual illustration of a hyperspectral image cube (hypercube) data. The x- and y-axis corresponds to the spatial width and height of the image and the third dimension is the spectral dimension (Hyperspectral Imaging for Thyroid and Salivary Gland Tumor Detection, 2020)....	10
Figure 1.2 The Handheld HSI scanner, LeafSpec (Wang et al., 2020).....	12
Figure 1.3 The NDVI heatmap of the HS images taken by LeafSpec. The resolution of the LeafSpec is high enough that the vein of the leaf can be resolved (Wang et al., 2020).	13
Figure 1.4 The Robotics system that automates the scanning process of LeafSpec (Chen et al., 2021).	14
Figure 2.1 LeafSpec Handheld HSC for dicot leaf (a) LeafSpec for dicot leaf picture (b) Internal structure of the LeafSpec for dicot leaf device.	16
Figure 2.2 HSC used in LeafSpec for dicot leaf (a) The internal structure of the camera. (b) A picture of the camera assembled.	17
Figure 2.3 The scanning mechanism of the LeafSpec uses a rack and pinion mechanism to drive the HSC back and forth to take the HS images of an entire leaf.	21
Figure 2.4 The mechanism for open and close LeafSpec uses a slider-crank mechanism. A servo is used to lift the lower case to the upper case.	22
Figure 2.5 The attachment to the robotic arm is located above the center of mass. The blue rectangle is the adapter to the sixth joint of the robotic arm.	23
Figure 2.6 The electrical system of the LeafSpec consists of voltage regulators, microprocessors, micro-controller, and peripheral for the microprocessor and micro-controller.	24
Figure 2.7 The data flow and management between the LeafSpec, smartphone, and computer ..	26
Figure 3.1 The NDVI heatmap of a soybean leaf shows the distribution of NDVI value is not uniform.	27
Figure 3.2 The plot shows a linear relationship between nitrogen content and the mean NDVI value of the leaf.	30
Figure 3.3 Correlation between N prediction and ground truth data using the mean NDVI modeling. The correlation has an R^2 of 0.805.	32
Figure 3.4 Correlation between N prediction and ground truth data using the NDVI heatmap distribution modeling. The correlation has an R^2 of 0.871.	33
Figure 4.1 The 6 DOF robotic arm with LeafSpec attached during leaf scanning.	35
Figure 4.2 The current UAV design using the selected parts.	36
Figure 4.3 Diagram of the electrical component on the UAV and the ground station.	40

ABSTRACT

Nowadays, soybean is one the most consumed crops in the world. As the human population continuously increases, new phenotyping technology is needed to help plant scientists breed soybean that has high-yield, stress-tolerant, and disease-tolerant traits. Hyperspectral imaging (HSI) is one of the most commonly used technologies for phenotyping. The current HSI techniques include HSI tower and remote sensing on an unmanned aerial vehicle (UAV) or satellite. There are several noise sources the current HSI technologies suffer from such as changes in lighting conditions, leaf angle, and other environmental factors. To reduce the noise on HS images, a new portable, leaf-level, high-resolution HSI device was developed for corn leaves in 2018 called LeafSpec. Due to the previous design requiring a sliding action along the leaf which could damage the leaf if used on a soybean leaf, a new design of the LeafSpec was built to meet the requirements of scanning soybean leaves. The new LeafSpec device protects the leaf between two sheets of glass, and the scanning action is automated by using motors and servos. After the HS images have been collected, the current modeling method for HS images starts by averaging all the plant pixels to one spectrum which causes a loss of information because of the non-uniformity of the leaf. When comparing the two modeling methods, one uses the mean normalized difference vegetation index (NDVI) and the other uses the NDVI heatmap of the entire leaf to predict the nitrogen content of soybean plants. The model that uses NDVI heatmap shows a significant increase in prediction accuracy with an R^2 increase from 0.805 to 0.871. Therefore, it can be concluded that the changes occurring within the leaf can be used to train a better prediction model.

Although the LeafSpec device can provide high-resolution leaf-level HS images to the researcher for the first time, it suffers from two major drawbacks: intensive labor needed to gather the image data and slow throughput. A new idea is proposed to use a UAV that carries a 6 degree of freedom (DOF) robotic arm with a LeafSpec device as an end-effect to automatically gather soybean leaf HS images. A new UAV is designed and built to carry the large payload weight of the robotic arm and LeafSpec.

1. INTRODUCTION

Soybean is one of the most valuable crops in the world. There are multiple uses for soybeans, such as oil extraction, livestock feeds, and aquaculture. Soybean is also a good source of protein and other nutrients for humans (Masuda & Goldsmith, 2009). Currently, the human population is expected to grow to over 9 billion by 2050 (Li et al., 2014). Because of the continuous increase in the human population and consumption of food per person, the global demand for food is expected to increase for the next 40 years (Godfray et al., 2010). However, the growth in agricultural production has not kept up with the population growth. It is projected the crop yield for soybeans will increase by 1.3 % per year which is not enough to accommodate the increase in demand (Pagano & Miransari, 2016). To ensure food security for human society, high-yielding and stress-tolerant plants need to be selected and bred. The advancement in techniques such as DNA sequencing allows plant scientists to molecularly breed plants. However, the lack of access to phenotyping capabilities hinders plant scientists' ability to relate genetics to the plant's growth, yield, and stress tolerance (Li et al., 2014).

HSI can be used to help plant scientists quantitatively choose the better breed of plants in a high-throughput and non-invasive manner (Gowen et al., 2007). In the traditional RGB camera, each pixel contains three values that correspond to the intensity of red, green, and blue color. In contrast, a hyperspectral camera (HSC) can capture a spectrum for each pixel. The number of the bands for the spectrum can vary from tens of bands to hundreds of bands. The setup of an HSI system consists of four parts: light source, objective lenses, an imaging spectrograph, and a grayscale camera. The light from the light source either reflects off or is transmitted through the plant surface into the HSC. As the light enters the HSC, it first passes through an objective lens which focuses the light onto the aperture of the camera. After the aperture, there is a spectrograph that uses a diffraction grating to split light into individual wavelengths. A diffraction grating can disperse the incoming light into its component wavelength, similar to how a prism disperses sunlight into a rainbow. Finally, the dispersed light is captured by a grayscale camera. Since each image captured by the grayscale camera contains one spatial and one spectral dimension, the HSC is a line-scanning camera. Either the object or the camera needs to move to capture the HS images of the entire object. The resulting data captured by the camera is called a hypercube as illustrated in Figure 1.1 (Mishra et al., 2017).

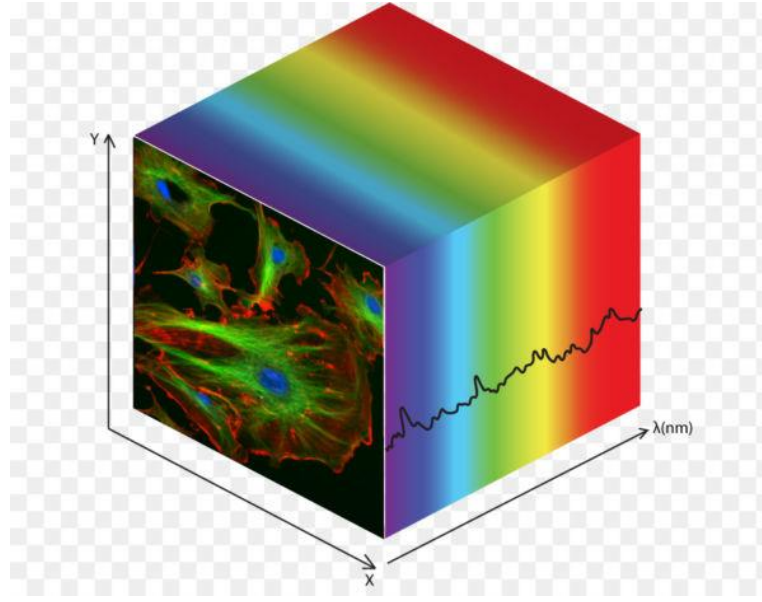


Figure 1.1 A visual illustration of a hyperspectral image cube (hypercube) data. The x- and y-axis corresponds to the spatial width and height of the image and the third dimension is the spectral dimension (Hyperspectral Imaging for Thyroid and Salivary Gland Tumor Detection, 2020).

1.1 Literature Review

1.1.1 Current Hyperspectral Imaging System in Agriculture

Hyperspectral imaging technologies have been applied in both greenhouses and fields. In greenhouses, the most popular method for collecting hyperspectral (HS) images was to enclose the entire plant inside an environmentally controlled box blocking all ambient light (Ge et al., 2016). To increase the throughput of the imaging system, the entire process was automated by attaching the imaging system to a conveyor belt (Ma et al., 2019). Another method for high throughput phenotyping system was to use an overhead crane system with an HSC mounted to capture top views of the plants (Virlet et al., 2017).

All of these HSI systems demonstrated their ability to predict nutrient content. However, there are three major sources of noise the systems could not avoid. The first source of noise comes from the relative angle between the leaf and the HSC. When the leaf is perpendicular to the HSC, the reflectance of the leaf is at its maximum. As the leaf angle deviates from the perpendicular position, the light intensity changes. If the same white reference is used to calibrate the HS images, the

calibration will not be accurate for a leaf that is not perpendicular to the camera. The second source of noise comes from specular reflection and shadows on the leaf. Specular reflection is a mirror-like surface reflection, and it can saturate the image and prevent the production of the desired spectrum. Similarly, shadows cause the spectrum to change since the incoming light source is not the same as the non-shadowed part of the plant. The last major source of noise comes from the variance between the top leaves and bottom leaves of the plant. The nutrient distribution throughout the plant is not uniform (Lavado et al., 2001). The signal from the variance between the leaves can overpower the signal of plant traits. The current method for processing the hyperspectral image is to average all the spectrums that correspond to the plant. Each plant is only represented by one spectrum which means the signal between different sections of the plant is lost from the averaging operation.

In the field, HSC has been installed on both aerial (Satellite, UAV, etc.) and ground platforms. The typical use of HSC on an aerial platform is on an unmanned aerial vehicle (UAV). There were many UVA platforms designed to carry an HSC. The lightweight UAV developed at the University of Jyväskylä had an interferometer-based HSC. The data from UAV was able to estimate biomass and nitrogen of wheat fields. The estimated normalized root mean squared error (NRMSE) was 18.1% and 19.7% for biomass and nitrogen respectively (Pölonen et al., 2013). HSC has also been used on ground-based vehicles for various applications. A team from The University of Sydney developed a ground base vehicle carrying an HSC used to estimate the maturity of mangoes. The cross-validation regression result showed the R^2 value was 0.74 for correlation between prediction and ground truth (Wendel et al., 2018).

The current setup of the field HSI system uses sunlight as the light source for the camera. Depending on the time of the day and the location of the field, the sunlight intensity and angle can change drastically (Ma et al., 2021). The normalized difference vegetation index (NDVI) of the plant follows a V-shaped pattern where the minimum is at solar noon time when the sun is at the highest location in the sky (Ma et al., 2021). Additionally, the resolution of a field hyperspectral camera can only achieve 10 mm spatial resolution after orthorectification (Kanning et al., 2018). Orthorectification is a process to remove the effect of image perspective (tilt) and relief (terrain) (*Orthorectification – OSSIM*, n.d.). With 10 mm spatial resolution, some of the pixels in the HS images will inevitably have the signal from plants and soil mixed which can decrease the signal to noise ratio of the HS images. Although the current HSI systems, in the greenhouse or the field,

have some noise source needing to be reduced, the advantage of using such systems is that it has a very high throughput. Also, the amount of labor needed to gather the data is very minimal, since most of the system is either autonomous or semi-autonomous.

1.1.2 Leaf-level HSI System

To reduce the noises when taking HS images, a handheld HSC, LeafSpec, was developed for maize plants to take leaf-level HS images. The goal of the LeafSpec was to minimize the noise sources such as leaf angle, leaf reflection, and ambient light differences. LeafSpec enclosed the scanning section of the leaf into a small dark room. This setup allowed the lights and other environmental factors to be well controlled (Wang et al., 2020). The light source for the HSC was two halogen lights which provided a stable smooth and monotonic spectrum (Mishra et al., 2017). Instead of the typical HSI setup which used reflectance imaging, the LeafSpec used transmittance imaging which provided better image quality by eliminating specular reflection (Wang et al., 2020). Because of the well-controlled environment during imaging, the LeafSpec HSC provided a high resolution of leaf-level HS images. An example of the HS images is shown in Figure 1.3.



Figure 1.2 The Handheld HSI scanner, LeafSpec (Wang et al., 2020)

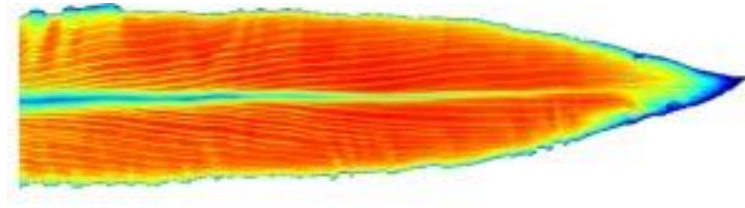


Figure 1.3 The NDVI heatmap of the HS images taken by LeafSpec. The resolution of the LeafSpec is high enough that the vein of the leaf can be resolved (Wang et al., 2020).

The design of LeafSpec required the operator to slide the device over the entire length of the leaf. This can be very labor-intensive as the operator operated LeafSpec in a heavily dense cornfield. The throughput of the LeafSpec HSC was much slower than the greenhouse HSC tower or remote sensing UAV in the field. To solve the problem, a new robotic system was developed to attach the LeafSpec as the end-effector. The robotics system used a machine vision system to detect the target leaf and a cartesian robotic manipulator to grasp the corn leaf using LeafSpec (Chen et al., 2021). The comparison between manually and automatically scanned HS images showed robotics systems can achieve gathering the same image quality compared to human operation (Chen et al., 2021). This system was able to successfully automate the process of scanning the leaves, but the average cycle time between each scan was 86 seconds which was still not comparable to the typical HSI systems (Chen et al., 2021).

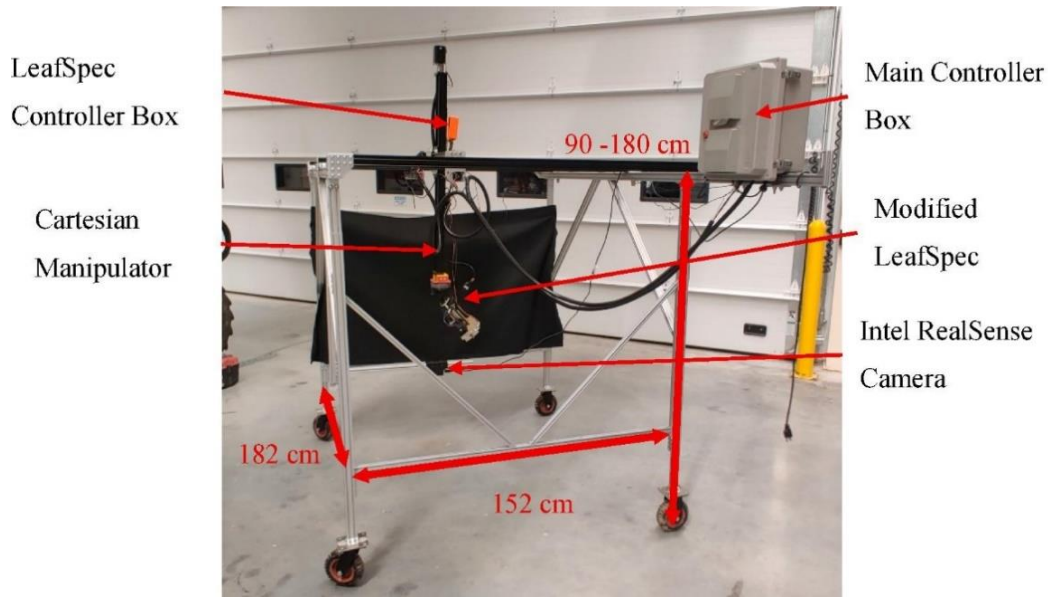


Figure 1.4 The Robotics system that automates the scanning process of LeafSpec (Chen et al., 2021).

1.1.3 Hyperspectral Image Modeling

After the HS images were acquired from HSC, the data needed to be analyzed and modeled to predict certain features of the plant such as nutrient content, yield, or disease detection. The size of the HS image data could be very large due to additional spectral dimensions. The first step of processing the data was to segment the plant pixels out of the entire HS images, then the spectrum of all plant pixels could be averaged to have one spectrum representing the plant (Mohd Asaari et al., 2018). There were typically two methods used to train the model from the spectrums, partial least square regression (PLSR) and deep learning neural network.

PLSR modeling works by projecting the predicted variables and the observable variable onto a latent space that can represent most of the variation in the given data. A linear regression model can be found in the latent space. The PLSR model has been used on the HS images collected by LeafSpec to predict nitrogen (N) content and relative water content (RWC) for corn plants. With 3 latent variables, the model achieved an R^2 of 0.88 and root mean squared error (RMSE) of 0.246 on predicting N content. The model also achieved an R^2 of 0.77 and RMSE of 0.049 for RWC (Wang et al., 2020).

In recent years, deep learning neural network models have become popular for HS image modeling to predict various plant traits. A new deep learning model was developed for nitrogen

prediction on oilseed rape (Yu et al., 2018). The paper introduced a deep learning model using the average spectrum of oilseed rape leaf as the input and predicted the nitrogen content of the plant as the output. The deep learning network consisted of a stacked auto-encoder (SAE) and a fully connected neural network (FNN). The SAE network was used to extract the features from the average spectrum. The FNN used a fully connected layer to predict the nitrogen content using the extracted features from SAE. The deep learning model produced a good correlation between the predicted nitrogen content and ground truth with an R^2 of 0.903 (Yu et al., 2018). From the NDVI heatmap in Figure 1.3, the spectrum response from the leaf is not uniform. The information on how the spectrum of the leaf changes at different locations might be able to produce a more accurate prediction of the plant trait.

1.2 Automatic Soybean Leaf-level Hyperspectral UAV

To reduce the noise in the current HSI system and increase the throughput of HS image gathering, a new project uses UAV to collect leaf-level HS images by hopping around the field. The project chose first to apply the technology on soybean instead of corn because soybean leaves are easier to manipulate with a 6 degree of freedom (DOF) robotic arm. In comparison, a cartesian manipulator is suitable for corn leaves (Chen et al., 2021), but a cartesian manipulator is hard to implement onto a UAV. This project consists of three parts which include:

1. A new LeafSpec device designed for soybean leaves.
2. A new robotic arm along with a machine vision system to carry the new LeafSpec device to gather soybean HS images.
3. A new UAV that can hop around a soybean field to collect leaf-level HS images using the robotic system.

In this project, the author mainly contributed to two parts of the project: developing the new LeafSpec HSC for soybean leaves for attachment to the robotic arm and configuring and building the new UAV for carrying all the equipment.

2. LEAFSPEC FOR DICOT LEAVES

2.1 Overview

The LeafSpec for soybean leaves was designed based on the LeafSpec for corn leaves by Dr. Wang (Wang et al., 2020). In the lightbox of LeafSpec for corn, there was a groove at the center to accommodate the midrib of corn leaves. The design also required the LeafSpec device to slide across the entire length of the leaf. If using the same LeafSpec device on a soybean leaf, the dragging force would break the fragile leaf.

Therefore, the LeafSpec for soybean leaves needs to avoid sliding across the leaf directly with the HSC. The design of the LeafSpec for soybean leaves uses two sheets of glass to compress the leaf in between and protect it from sliding damage. The HSC and the lightbox are aligned on the opposite side of the glass sheets with a motor driving the entire imaging set up across the leaf using a rack and pinion mechanism. The internal structure of the LeafSpec device is shown in Figure 2.1. In addition to the LeafSpec device, a smartphone APP is needed to receive previews of the HS images, and the user uses the smartphone to command the LeafSpec device to save the full HS images and the metadata of the HS images.

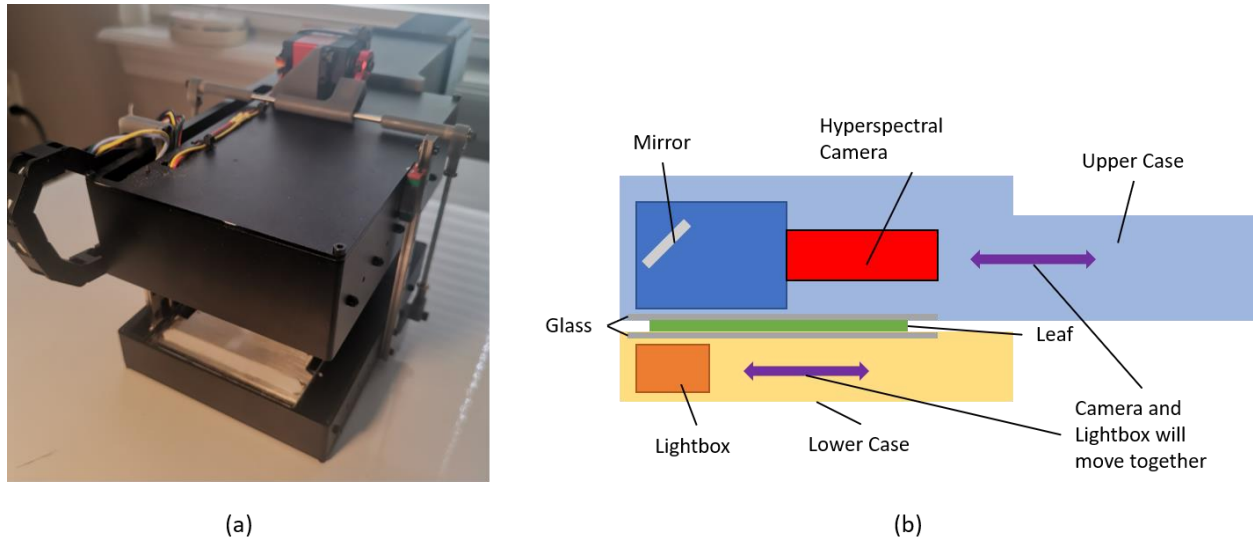


Figure 2.1 LeafSpec Handheld HSC for dicot leaf (a) LeafSpec for dicot leaf picture (b) Internal structure of the LeafSpec for dicot leaf device.

2.2 Hardware Design

2.2.1 Hyperspectral Camera

The HSC used in the LeafSpec for soybean leaves was the same as the HSC used in LeafSpec for corn leaves. In hyperspectral imaging for agricultural application, the red edge (RE, 670-780 nm) in the spectrum is used to model the plant stress, nutrient content, and chlorophyll content. The HSC in LeafSpec needs to operate in both visible and near-infrared (NIR) bands. The operating range for the HSC needed to be between 450 nm to 900nm. The HSC consists of collecting lens, slit, filter, collating lens, grating, focusing lens, and imaging sensor. The details of the individual components will be explained in the sections below.

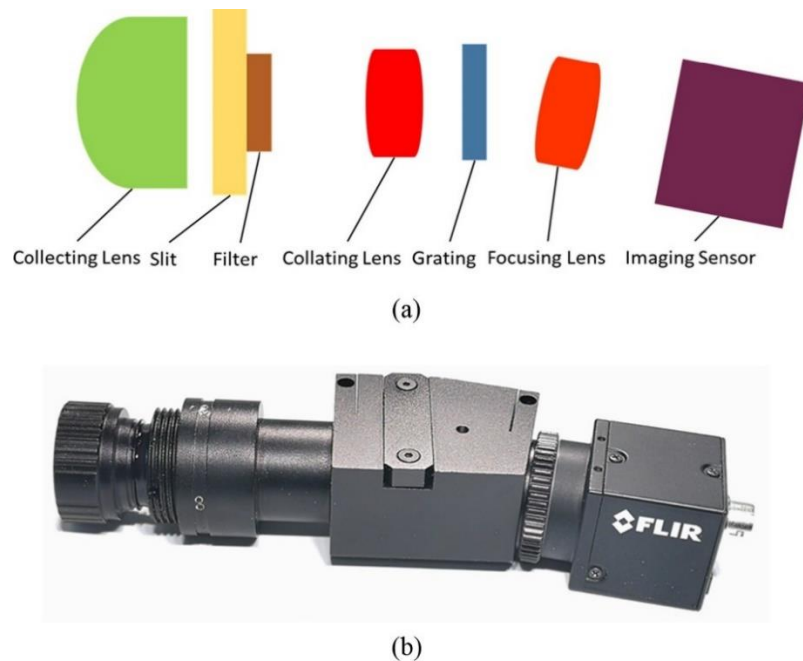


Figure 2.2 HSC used in LeafSpec for dicot leaf (a) The internal structure of the camera. (b) A picture of the camera assembled.

Diffraction Grating and Filter

The role of the diffraction grating is to separate the incoming polychromatic light into monochromatic light (Palmer, 2005). The diffraction grating the HSC uses is a transmission grating (GT13-03) from Thorlabs Inc. The grating has 300 grooves per millimeter with a groove angle of 17.5 degrees. The physical dimensions of the grating are 12.7 mm x 12.7mm. The

transmittance of the grating has a range of 38% to 74% between the 450 nm and 900nm light. The diffraction angle of the grating is 11.35 degrees using Equation 1.

$$n\lambda = d(\sin\theta + \sin\theta') \quad \text{Equation 1}$$

where n is the diffraction order, λ is the wavelength of the monochromatic light, d is the groove spacing, θ is the groove angle, and θ' is the diffraction angle (Palmer, 2005).

Since only the first-order diffraction pattern is needed for the HSC, a filter is required to remove the light with a wavelength under 440 nm because it can create a second-order diffraction pattern. The filter used in the HSC is a long-pass filter (62-975) from Edmund Optics. The transmission efficiency of the filter is over 91% between the range of 458 nm to 1600 nm (Wang et al., 2020).

Lenses and Slit

The slit inside the HSC acts as an aperture in a traditional RGB camera, limiting the amount of light passing through. The slit (S50RH) from Thorlabs Inc. has a physical dimension of 50 microns wide and 3 mm long. Since the slit is a rectangular shape, the slit only allows one line of light through.

There are three lenses used in the HSC: collecting lens, collating lens, and focusing lens. The collecting lens focuses the light transmitted through the leaf onto the slit. In the LeafSpec HSC for corn leaves, a 2.8 mm focal length collecting lens was used (Wang et al., 2020). However, to reduce the warping at both ends of the scanning line, a 4 mm focal length collecting lens is used in the LeafSpec for soybean leaves. The purpose of the collating lens is to convert the light exiting the slit into parallel light so the light can be diffracted using the diffraction grating. The purpose of the focusing lens is to focus the monochromatic light from the diffraction grating onto the imaging sensor (Wang et al., 2020). For both the collating and focusing lens, an achromatic doublet (#63-720) from Edmund Optics was used with a focal length of 30 mm and a diameter of 10 mm.

Imaging Sensor

The imaging sensor that was used in the HSC is a monochrome camera (BFLY-U3-05S2M-CS) from Teledyne FLIR. A monochrome camera is needed because the HSC is a line scanning camera. For each pixel in the image, it represents the intensity of a wavelength at a certain position on the line. The imaging sensor is equipped with a Sony CCD with a global shutter. The imaging sensor uses USB 3.1 for power and data transfer. The full specification of the imaging sensor is listed below:

Table 2.1 Full specification of the imaging sensor (BFLY-U3-05S2M-CS) from Teledyne FLIR

Parameter	Setting
ADC	12-bit
Chroma	Mono
Maximum Frame Rate	50
Megapixels	0.5
Quantum Efficiency	81% (at 525 nm)
Readout Method	Global Shutter
Resolution	808 x 608
Sensor Format	1/3"
Sensor Name	Sony ICX693
Sensor Type	CCD
Dynamic Range	66.87 dB
Saturation Capacity (e-)	22074
Interface	USB 3.1 Gen 1
Power Consumption	3W

2.2.2 Lightbox

One of the major noise sources for the current HSI system, mentioned in section 1.1.1, is the effect of lighting changes between images. To eliminate this noise, the LeafSpec device encloses the leaf in a dark chamber. The light source of the HSC is the lightbox on the opposite side of the leaf which is installed with two 12W halogen lights. Halogen lights are chosen because the light it

emits covers a wide range of wavelengths from visible to infrared (IR) with a very smooth spectrum. Since the HSC is a line scanning camera, the lightbox is designed to only illuminate a narrow and long section of the leaf. A Teflon sheet covers the outlet of the lightbox to diffuse light across the entire illuminating section. The lightbox was made with aluminum with a mirror-like finish inside. The mirror finish allows the light to reflect effectively inside the lightbox which increases the brightness of the light output.

2.2.3 Scanning Mechanism

The scanning mechanism consists of a rack and pinion mechanism, two sheets of glass, and a drive motor with an encoder. In the original LeafSpec device made for corn, the HSC was mounted vertically with respect to the leaf. If the current version of LeafSpec uses the same design, the total volume of the case required will be very large. Alternatively, a mirror is used to reflect the light 90 degrees, so the HSC could be placed parallel to the scanning bed. The leaf is pressed between two sheets of glass to protect the leaf from sliding damage from the HSC. The two sheets of glass flatten the leaf to eliminate the noise caused by the leaf slope.

There are several choices for a linear actuation mechanism, such as lead screw, rack and pinion, belt drive, and chain drive. The rack and pinion mechanism is chosen because of its small size and simple setup. The entire actuation mechanism fits inside the case of the HSC. All the other mechanisms need to be mounted outside the case of the HSC and connected to the HSC via an opening on the case, which will allow ambient light to leak into the device and compromise the image quality. The illustration of the rack and pinion setup inside LeafSpec is shown in Figure 2.3. The module of the rack and pinion is 0.8 which gives fine control of the position as well as allows for larger tolerance during assembly. The pinion has 20 teeth with a pitch diameter of 16 mm.

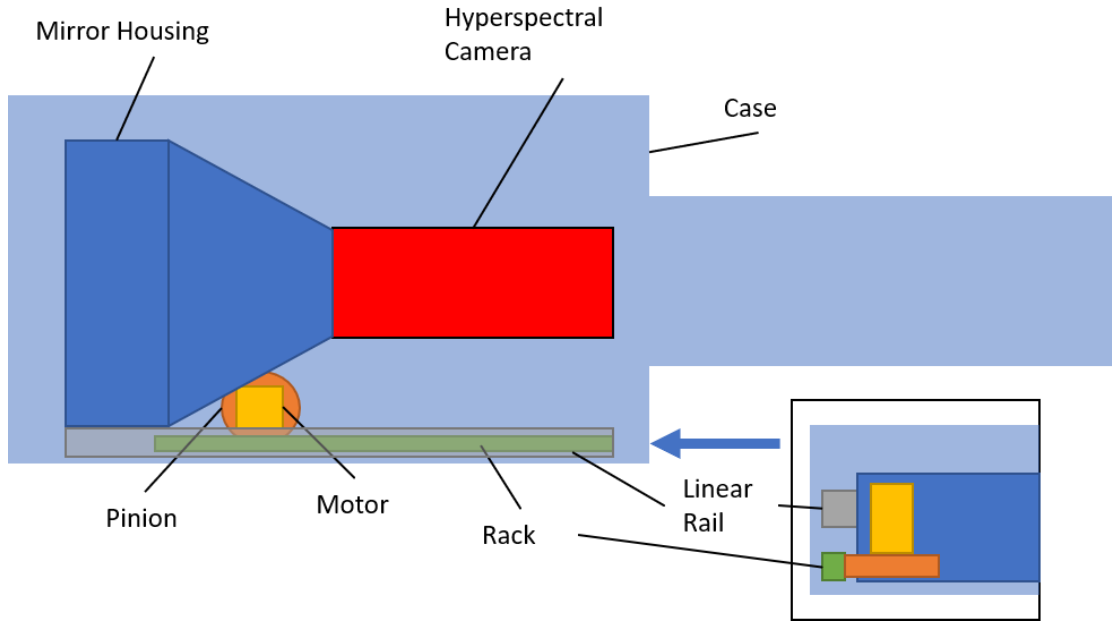


Figure 2.3 The scanning mechanism of the LeafSpec uses a rack and pinion mechanism to drive the HSC back and forth to take the HS images of an entire leaf.

The motor chosen to drive the entire system is a micro metal gear motor with a 1000:1 gear ratio. The motor has a physical dimension of 29.5 mm x 10 mm x 12 mm (length x width x height) and a weight of 10.5 grams. The motor produces a maximum torque of 11 kg·cm which is enough to drive the entire system.

2.2.4 Device Open/Close Mechanism

The objective of the overall project was to attach the new LeafSpec device to a robotic arm and automatically scan the leaf-level HS images, so the opening and closing of the upper and lower case needed to be automated. A servo with a slider-crank mechanism is used to open and close the device when grasping the leaf. The speed of the current design is much faster than a linear actuator because the servo angle can be easily controlled by a pulse width modulation (PWM) signal.

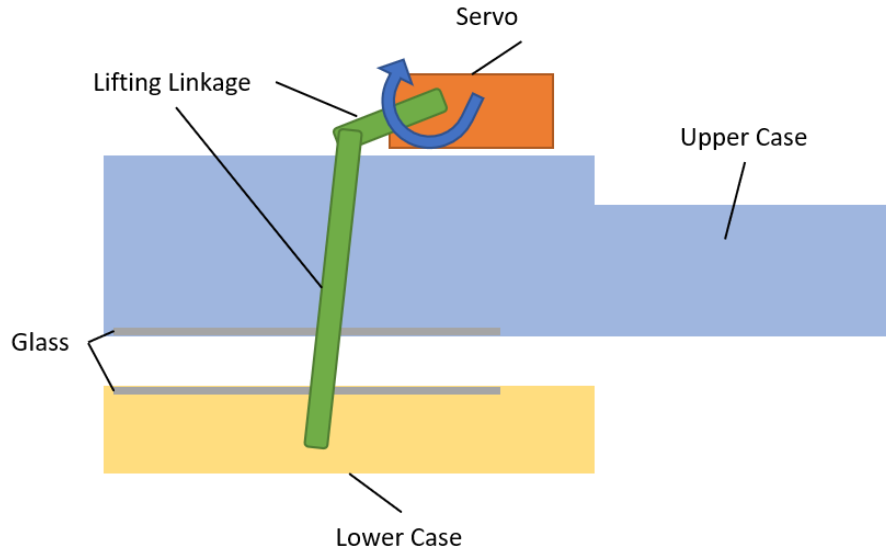


Figure 2.4 The mechanism for open and close LeafSpec uses a slider-crank mechanism. A servo is used to lift the lower case to the upper case.

2.2.5 Attachment to Robotic Arm

The robotic arm used in this project is OpenMANIPULATOR-P (RM-P60-RNH) made by Robotis Inc. The maximum payload for the robotic arm is 3 kg and the weight of the LeafSpec device is 2 kg. Because of the relatively heavy weight of the LeafSpec device, the positioning of the LeafSpec device is critical to the operation of the robotic arm. If the center of mass of the LeafSpec is not located along the centerline of the last joint of the robotic arm, there will be an additional moment around the centerline which adds additional load to the motors on the robotic arm. Since the center of mass is located at the same location for the servo, the attachment point needed to move above the servo to give clearance to the lifting mechanism. An arch was designed to attach at each end of the device to provide enough support when the HSC is at two extreme locations.

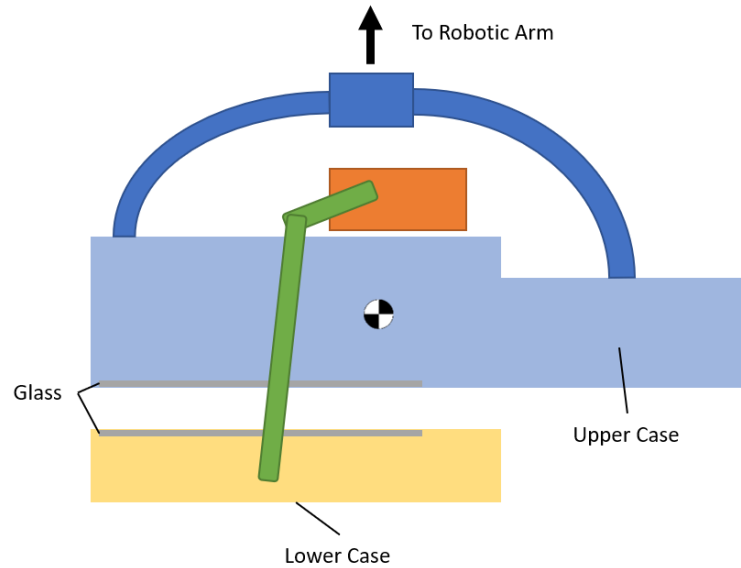


Figure 2.5 The attachment to the robotic arm is located above the center of mass. The blue rectangle is the adapter to the sixth joint of the robotic arm.

2.2.6 Electronics

In the new LeafSpec for soybean leaves, there are three sections in the electronic system: the power supply, microprocessor, and microcontroller. The power supply regulates the input voltage of 24V to 12V and 5V. The microprocessor is the brain of the operation; it interfaces with a camera, micro-controller, and Bluetooth module to communicate with a smartphone. The microprocessor also processes the incoming image data from the camera into HS images. The micro-controller receives commands from the microprocessor to actuate the mechanism and lights inside the device. In Figure 2.6, the diagram shows how the entire electronic system connects.

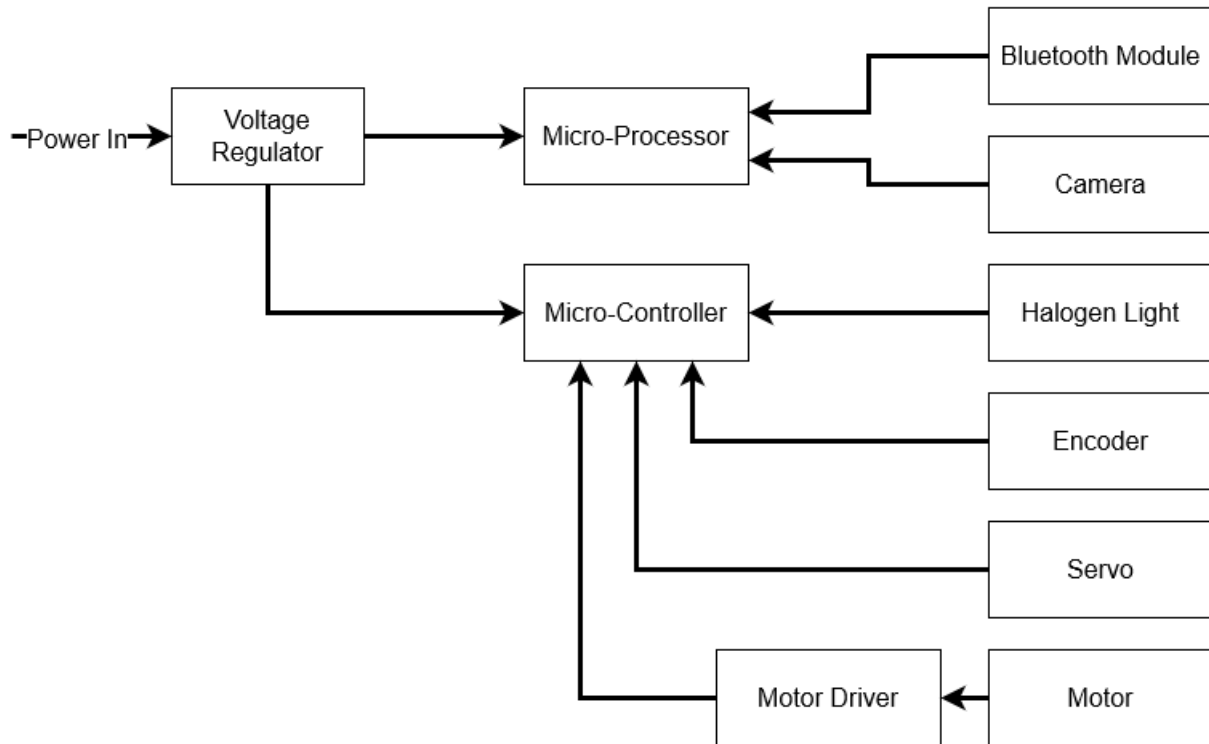


Figure 2.6 The electrical system of the LeafSpec consists of voltage regulators, microprocessors, micro-controller, and peripheral for the microprocessor and micro-controller.

Power Supply

The LeafSpec accepts 24 VDC as input voltage and reduces the current from the battery to the device. The robotic arm also uses 24 VDC as power. Since the battery voltage changes over time, two voltage regulators are needed to provide steady voltage for the electrical systems of the LeafSpec device. One of the voltage regulators transforms the 24 VDC to 12VDC for powering the halogen light. Another voltage regulator transforms the power from 24VDC to 5V DC to power the microprocessor, micro-controller, and all their peripherals.

MicroProcessor

The microprocessor of the LeafSpec acts as the brain of the entire operation. It handles the computation and storage of data, communication with a smartphone over Bluetooth, and sends commands to the microcontroller. This new version of LeafSpec uses a Raspberry Pi 4 as the microprocessor. The Raspberry Pi 4 has 4 GB of RAM to temporarily store image data from the

imaging sensor during scanning. The Raspberry Pi has a Bluetooth module attached to send scan information and receive commands from a paired smartphone which is the user interface of the LeafSpec device. The Raspberry Pi communicates with the microcontroller via Universal Asynchronous Receiver-Transmitter (UART).

MicroController

The microcontroller in the new version of LeafSpec actuates all the mechanisms and turns on/off the halogen lights. The LeafSpec uses an Arduino nano as the micro-controller. An Arduino was chosen because it has hardware PWM which provides a clean signal to control the motor and servo when under load. In contrast, the PWM signal from the Raspberry Pi 4 is simulated using software that is not reliable under load, and it also requires significant computation time to generate the PWM signal. The Arduino controls the motor by using an H-bridge motor controller which uses two PWM signals to control the speed and direction of the motor. An Arduino also has hardware interrupts which are important for sensing encoder signals at high speed. On the micro gear motor, there is a magnetic encoder that uses two hall-effect sensors. The encoder has a resolution of 12000 counts per revolution which means the encoder has a 0.004 mm special resolution, whereas the Raspberry Pi's software implementation of interrupts is not fast enough for sensing encoder signals. To limit the range of the HSC scanning area, two limit switches are used and connected to the Arduino. The halogen lights are controlled using a p-channel MOSFET (IRF520) because lights will draw about 2A of current when turned on.

2.3 Device Operation and Data Flow

To operate the LeafSpec device, an Android smartphone is needed for previewing the HS images taken by the LeafSpec device and allowing the user to input the metadata of the current HS images. The smartphone connects to the LeafSpec device using Bluetooth. The diagram in Figure 2.7 shows how the data flows between different components of the LeafSpec system.

The LeafSpec device can be triggered to start scanning by using a push-button for manual operation or a relay for autonomous operation. The Raspberry Pi initializes the HSC and sends a command to the Arduino to close the LeafSpec device and start spinning the motor. The motor runs continuously until reaching the limit switch. After the motor has started spinning, the

Raspberry Pi starts acquiring images from the HS images for each line until the HSC has reached the end of the scanning bed. As soon as an image has been received, the Raspberry Pi requests the current distance from the Arduino and then stores the image in RAM for later processing after the scanning has been completed. Once the scanning has been completed, the Arduino moves the HSC back to its original position. Meanwhile, the Raspberry Pi processes the data by organizing the images into a single hypercube. The Raspberry Pi also generates an NDVI heatmap for showing as a preview on the smartphone. The user can then choose to save or discard the data on the smartphone. The full HS images hypercube data is saved on the SD card installed on the Raspberry Pi. For further processing HS images and using the data to model, the SD card can be read by a computer.

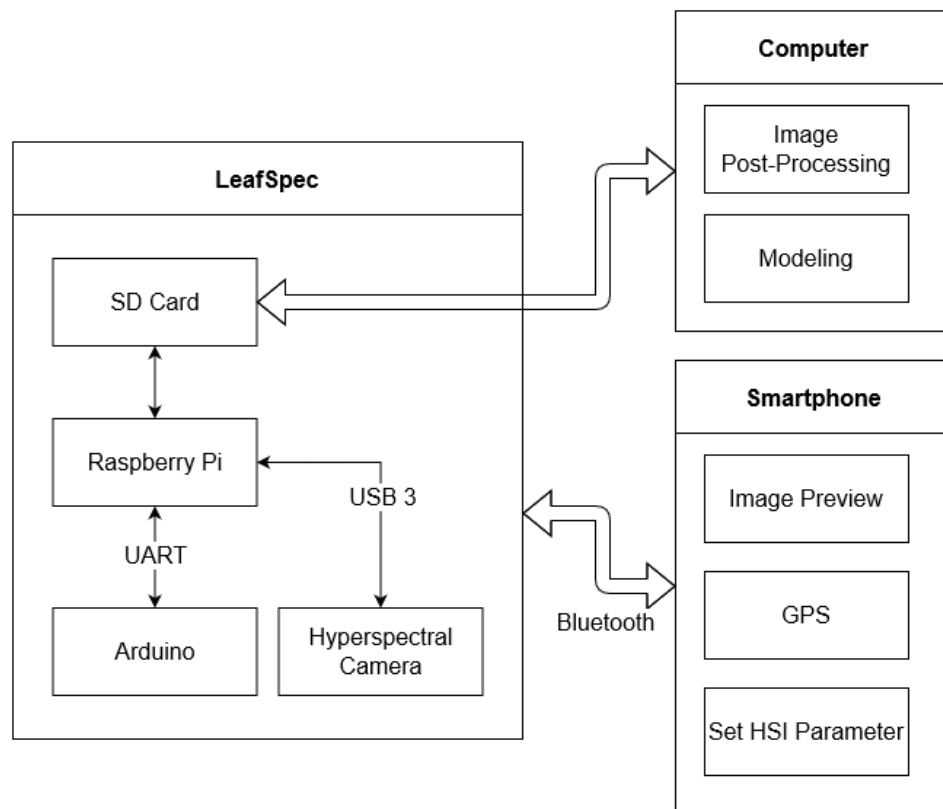


Figure 2.7 The data flow and management between the LeafSpec, smartphone, and computer

3. HS IMAGES MODELING USING LEAF NDVI DISTRIBUTION

3.1 Overview

As mentioned in the literature review, the current method for modeling using HS images was by averaging all the plant spectrum into one spectrum. Figure 3.1 shows the NDVI heatmap of a soybean leaf taken by the new LeafSpec device. One observation made is the distribution of the spectrum is not uniform. For example, the NDVI value at the edge of the leaf is lower than the center of the image. When taking a closer look, as the pixels get further from the veins of the leaf, the NDVI value drops.

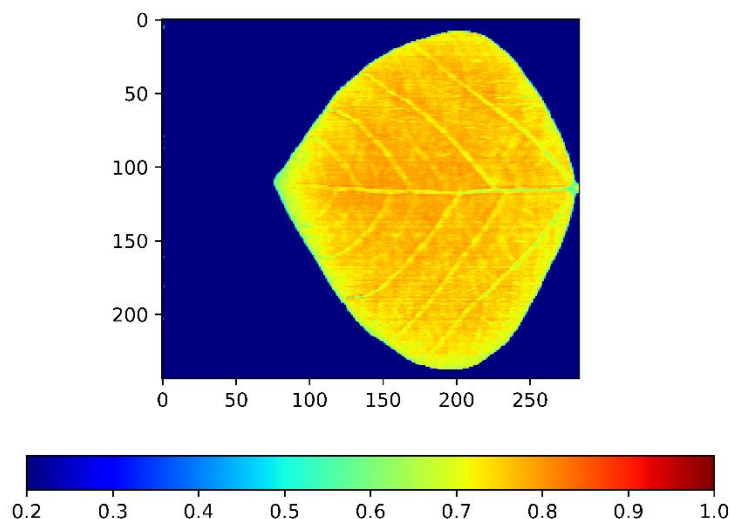


Figure 3.1 The NDVI heatmap of a soybean leaf shows the distribution of NDVI value is not uniform.

In this chapter, two methods of training a nitrogen prediction model were used to compare their performance. The first method used the mean spectrum of the entire leaf to calculate the mean NDVI of each leaf as the input to predict the nitrogen content of the soybean plant. The first method uses a linear regression model for the prediction. In the second method, the NDVI heatmaps are used to train the model using a deep learning neural network.

3.2 Data collection

3.2.1 Experiment Setup

The experiment for collecting HS images to train the nitrogen prediction model was conducted in the Purdue Lilly greenhouse in December 2020. A total of 64 soybean plants were grown under supplemental lighting for 10 hours a day. The 64 plants were evenly split between two genotypes: Pioneer P34T21SE and Thorne. For each genotype, the 32 plants were split into four different treatment groups: 8 plants with high N treatment and well-watered, 8 plants with high N treatment and drought-stressed, 8 plants with low N treatment and well-watered, and 8 plants with low N treatment and drought-stressed. The medium used in the experiment was a mix of 67% Metro Mix 510 (Sun Gro Horticulture) and 33% Greens Grade™ (Profile®) by volume. The N treatment was applied one week after transplanting the soybean seedling from plate to plot. The treatments were applied twice, one week apart. The concentration of the fertilizer used in the high N treatment plants was 200 ppm and 25 ppm for the low N treatment group. Initially, all plants were irrigated as needed. Four days before the sampling date, the irrigation for the drought-stressed plants was stopped.

3.2.2 HS images Collection

The sampling date was chosen to be December 17th, 2020, from 1:30 PM to 5:00 PM. For each plant, the top matured trifoliolate was imaged by the new LeafSpec device since it has been shown there are no significant differences in nitrogen content and relative water content (RWC) between the three leaves in a trifoliolate (Samantha, 2020). Each leaf in the top matured trifoliolate was imaged separately by cutting the leaf off the plant and scanned. In total, one hundred and ninety-four HS images were collected from the experiment.

3.2.3 Ground Truth Data Collection

To measure the N content, the entire plant from the soil and above was cut and placed in a paper bag. All the plants were then dried using a dryer until all water had been evaporated. The dried plants were then ground to a fine powder and sent to A&L Great Lakes Laboratories for N content analysis.

3.3 Modeling Steps

3.3.1 Pre-processing and Modeling Setup

Before HS images taken by the LeafSpec can be used for modeling, white referencing calibration and leaf segmentation need to be completed. The raw HS images need white reference calibration to get the transmittance of the leaf because there are non-uniformities in the LeafSpec imaging system. First, the imaging sensor sensitivity is not uniform across all wavelengths. Second, the light source, which is the two halogen lights, does have a uniform spectrum across wavelengths. Lastly, although a Teflon sheet was used in the lightbox to diffuse the two halogen lights, there are still lighting variations across the width of the scanning line. The white reference calibration picture is taken at the beginning of the experiments by turning on the halogen light for 2 seconds and acquiring one image from the imaging sensor. The 2 seconds wait time allows the spectrum from the halogen light to reach a steady state. For each line scanned by the HSC, a white reference calibration is needed. The transmittance can be calculated by dividing the raw HS images by the white reference pixel by pixel as shown in Equation 2.

$$transmittance = \frac{raw\ data}{white\ reference} \quad \text{Equation 2}$$

After the HS images have been calibrated using white reference, the leaf pixels were segmented by using the NDVI heatmap. The heatmap was calculated by applying the NDVI equation (Equation 3) to each spectrum in the HS images. The leaf could then be segmented using an NDVI threshold of 0.4.

$$NDVI = \frac{NIR - RED}{NIR + RED} \quad \text{Equation 3}$$

where NIR is the intensity of the spectrum at 840 nm and RED is the intensity of the spectrum at 640 nm.

For the two methods of modeling that will be discussed, the training dataset was the two of three leaves in the top matured trifoliate (128 HS images total). The testing dataset was the last leaf in the trifoliate (64 HS images total).

3.3.2 Modeling using Mean NDVI

The mean NDVI of the leaf was calculated using the segmented NDVI heatmap. By averaging all the NDVI values in the leaf pixels, one NDVI value represented one HS image. The mean NDVI value of each leaf against the N content ground truth was plotted, as shown in Figure 3.2. From the plot, a linear relation can be seen between the N content ground truth and the mean NDVI value of the leaf.

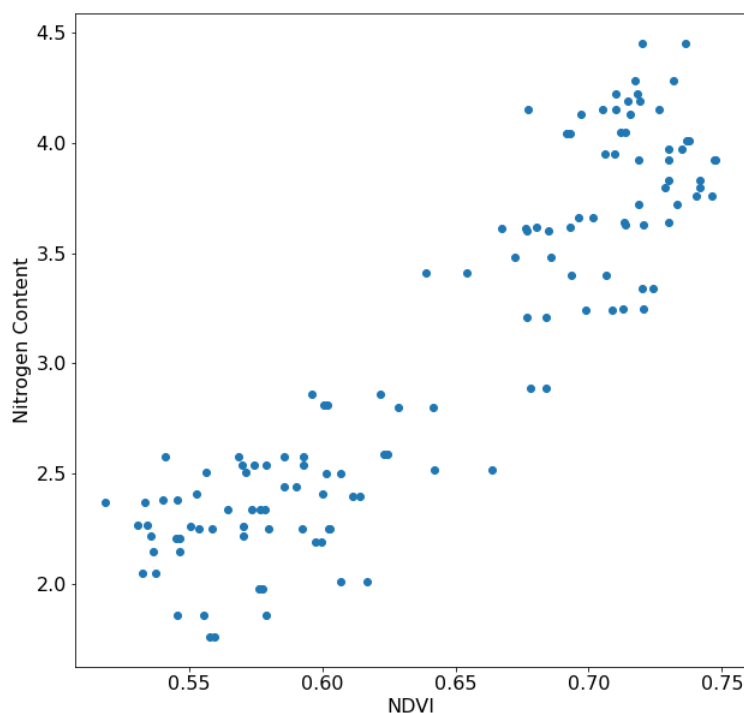


Figure 3.2 The plot shows a linear relationship between nitrogen content and the mean NDVI value of the leaf.

3.3.3 Modeling using Leaf NDVI Heatmap

To utilize the NDVI distribution across the entire leaf, a deep learning neural network known as ResNet-34 was used to model the N content of the soybean plants. In comparison with the traditional convolutional neural network (CNN), ResNet allows for a deeper network for the model to learn more detailed and abstract relationships within the training dataset. The ResNet uses a residual network as the building block of the network and has been shown to be easier to optimize.

The ResNet can also achieve higher accuracy while keeping the number of parameters in the model low (He et al., 2016). In the current application of N content prediction, a variant of ResNet, ResNet-34, was used. This network was chosen because it has the lowest number of parameters out of all the variants. Keeping the number of parameters low is important because the training dataset is small.

The ResNet-34 was originally developed for image recognition for RGB images. A modification was needed on the network to accommodate the NDVI heatmap which was used as a grayscale image. To modify, the number of input channels of the first 2D convolution layer was changed to one for the grayscale input image. The output of ResNet was a tensor with a size of 1000. A fully connected layer was needed to reduce the tensor to the size of 1, which was the nitrogen prediction. The loss used for training is a mean squared error (MSE) loss which has the formula shown in Equation 4.

$$l_n = (x_n - y_n)^2 \quad \text{Equation 4}$$

Where:

n is the batch index.

x is the input.

y is the reconstructed output.

Before the training dataset was used to train the model, all the NDVI heatmaps were normalized to a mean of 0 and a standard deviation of 1. The normalization allowed all the data to be on a common scale, so the model can be trained on the distribution within the image and not the differences in the range of values.

3.4 Modeling Result

3.4.1 Mean NDVI Modeling Result

A linear regression model was trained using the training dataset. The equation of the linear regression is:

$$N \text{ content} = 9.897 * NDVI - 3.316 \quad \text{Equation 5}$$

The linear regression model was then applied to the testing dataset and the correlation between the prediction and the ground truth data was plotted, as shown in Figure 3.3. The correlation had an R^2 of 0.805 and a root mean squared error (RMSE) of 0.338. The strong correlation showed the mean NDVI value of the leaf could be a good predictor for the N content of the entire plant.

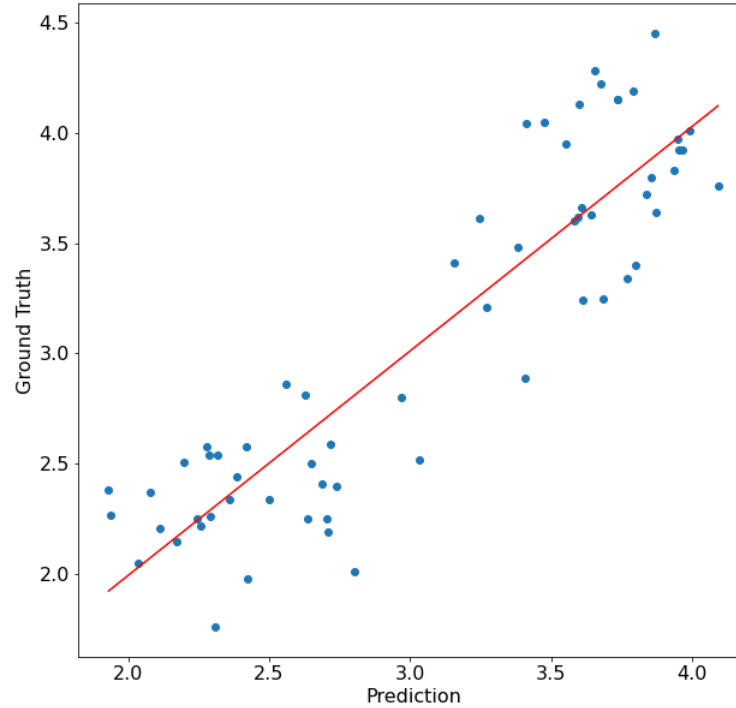


Figure 3.3 Correlation between N prediction and ground truth data using the mean NDVI modeling. The correlation has an R^2 of 0.805.

3.4.2 NDVI Heatmap Distribution Model Result

The deep learning model was trained on the training dataset over 50 epochs. Similar to the mean NDVI modeling, the model was applied to the test dataset and correlation analysis was performed on the predicted N content. The scatter plot of the test dataset ground truth and prediction is shown in Figure 3.4. The results show the correlation between the ground truth and predicted N content had an R^2 of 0.871 and RMSE of 0.276. There was a significant improvement in the R^2 value and the RMSE. This showed the model prediction could increase when the model considers the non-uniformity of the leaf.

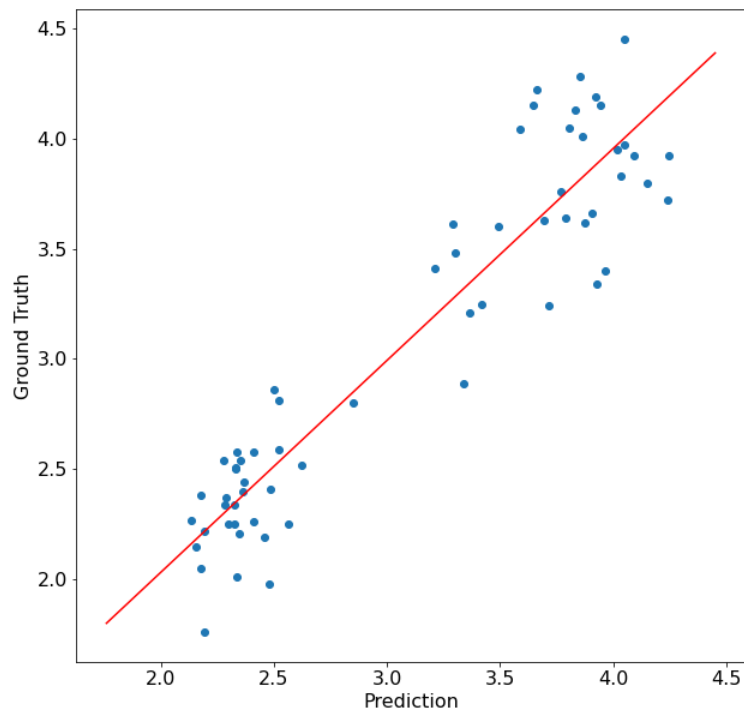


Figure 3.4 Correlation between N prediction and ground truth data using the NDVI heatmap distribution modeling. The correlation has an R^2 of 0.871.

4. UAV FOR IN-FIELD LEAF-LEVEL HYPERSPECTRAL IMAGE COLLECTION

4.1 Overview

The objective of the UAV is to carry the robotic arm, along with the new LeafSpec device for soybean leaves as a payload to collect leaf-level HS images in the field. The UAV allows the LeafSpec to quickly sample leaves at various spots in a large field autonomously. The designed workflow of the UAV starts before the UAV takes off. A flight plan containing the list of locations in the field needs to be loaded onto the UAV. For each location in the flight plan, the UAV will carry the robotic arm and LeafSpec to the target location and land on top of one row of soybean plants. The machine vision system on the robotic arm will find a top-matured leaf that can be reached by the robotic arm. The LeafSpec will scan the target leaf carried by the robotic arm. Lastly, the UAV will then take off and move to the next location.

At the beginning of this project, the plan was to purchase an off-the-shelf UAV designed for spraying in agriculture and then modify the UAV for the needs of the project. One of the most popular UAVs was the AGRAS T16 from DJI. However, the flight controller inside off-the-shelf UAVs was not open source which made modifying the UAV impossible. The plan for the project then changed to configuring the UAV using an open-source flight controller called ArduPilot. All hardware used in the project would be compatible with the ArduPilot software.

4.2 Current Progress

While the new LeafSpec for soybean leaves was developing, the 6 DOF robotic arm with machine vision was also developing by Ziling Chen. Before attaching the entire robotic system onto the UAV, an experiment that simulated UAV operation was conducted in the Purdue Lilly Greenhouse. The greenhouse has an overhead gantry that had previously used for simulating remote sensing applications. The robotic arm was attached to the gantry as shown in Figure 4.1. The plants used in the experiment follow the same planting procedure as described in Section 3.2.1. For each plant, the gantry will move the robotic arm to the plant location. The machine vision system will detect the location of the center top matured leaf. The robotic arm moves the LeafSpec to the leaf for gathering an HS image. From the experiment, the machine vision system achieved

a detection success rate of 89.2%. The robotic arm achieved a scanning success rate of 89.9%. Because of the high success rate from the experiment, the machine vision system and the robotic arm are ready to be installed on the UAV platform.

Meanwhile, the parts for the UAV have been bought and built. The first version of the UAV is shown in

Figure 4.2. All flight controller hardware is mounted at the center of the drone. Two batteries are mounted on each side of the drone to provide better balance. After the UAV has been assembled and loaded with software. The UAV was able to take off for the first time in May 2021.



Figure 4.1 The 6 DOF robotic arm with LeafSpec attached during leaf scanning.



v

Figure 4.2 The current UAV design using the selected parts.

4.3 UAV Configuration

The configuration of the UAV is shown in Table 2.1. The weight of each component is also shown in

Table 4.1. Due to the federal regulation on the weight of the UAV, the total weight of the UAV needs to be less than 55 lbs. The current configuration is estimated to have a takeoff weight of 37.618 lbs. which is less than the federal regulation and additional modifications can be made to further improve the UAV.

Table 4.1 List of parts on the UAV with the corresponding weight.

	Name	Part Description	Amount	Weight/unit (kg)	Total Mass (kg)	Total Mass (lb.)
Drone	Airframe	EFT E610	1	5.000	5.00	11.023
	Motor	DJI E5000	6	0.327	1.96	4.325
	Flight Controller	Pixhawk Cube Orange Standard Set	1	0.65	0.65	1.433
	GPS	Here 2+ GPS & RTK	1	0.05	0.05	0.11
	Battery	Tattu 6S LiPo 10000 mAh Battery	2	1.36	2.72	6.0
	Radio	FrSky Taranis Compatible Receiver X8R	1	0.018	0.018	0.04
	Data Link	RFD 900x Modem	1	0.014	0.014	0.03
Payload	Onboard Computer	Jetson AGX Xavier Developer Kit	1	0.65	0.65	1.430
	Robotic Arm	OpenMANIPULATOR-PRO	1	4.0	4.00	8.818
	HSC	LeafSpec	1	2.0	2.00	4.409
					Total Mass (lb.)	37.618

Table 4.2 List of parts for the ground station

Name	Part Description
Computer	Windows Laptop
Data Link	RFD 900x Modem
RTK	Here 2 RTK Ground Station
Controller	Taranis X9D Plus

4.3.1 Motor and Power

The motor for the UAV is the E5000 motor from DJI. The motor has the electronic speed controller (ESC) and propeller all built-in, making installation easier. The recommended takeoff weight for each motor is between 4.5 kg and 7kg. If six motors are used, the motors will be able to provide enough thrust to lift 36kg (80 lbs.) which is plenty for this project. The extra lift capacity also provides redundancy for the UAV if any motor fails. The motor requires a nominal voltage of 44.4V which is equivalent to a 12S LiPo battery. To achieve the 44.4V voltage, two 6S LiPo batteries were connected in series. According to the datasheet of the E5000 motor, the average power consumption for the motors is expected to be around 4500W during take-off and 3000W during hovering. On average, the power consumption is expected to be at 3400W, and the total battery capacity is 444 Wh. The overall flight time is expected to be around 10 minutes.

4.3.2 Airframe

The airframe used in the project is a hexacopter drone frame. It has an arm span of 1628mm which is far enough for the propeller to not be in contact with each other while the motor is spinning. The large footprint also allows us to design a large landing skid to accommodate the large robotic arm and LeafSpec system. Each arm of the airframe can be folded for easy transportation.

4.3.3 Flight Controller

The flight controller used on the UAV is the Cube Orange on an Automatic Dependent Surveillance-Broadcast (ADS-B) enabled board. This flight controller has one of the most powerful processors onboard with redundancies. It also has a built-in inertial measurement unit (IMU). The controller has enough inputs/outputs (IO) to add additional peripheral hardware to the UAV.

The global positioning system (GPS) receiver installed on the drone is the Here2 GPS receiver. The Here2 GPS module has a Real-Time Kinematic (RTK) feature. If an RTK ground station was set up, the Here2 module could provide 2.5 cm positioning accuracy. The centimeter-level accuracy is necessary because the drone needs to land on top of one row of the soybean plant, leaving only 15 cm of room for error.

4.3.4 Communication

There are two communication radios onboard. The first radio receiver is for manual control. By the Federal Aviation Administration (FAA) regulation, all UAVs need to have the ability to change from automatic to manual control mode at any time during the flight. The receiver used on the UAV is the FrSky X8R paired with the Taranis X9D Plus transmitter. This set of radios is only for controlling the UAV or switching it to manual mode. The second radio is for sending information about the UAV and the robotic arm back to the ground station. A pair of RFD900x modems were used. The radio has a range of 40 km and has a maximum air data transfer rate of 750 kbit/s. This radio is used to program flight plans, check the status of the UVA, and receive information about the HS images scanned.

4.3.5 Ground Station

The ground station consisted of a laptop, an RFD900 modem, a FrSky X8R transmitter, and an RTK ground station. The function of the last three parts was discussed in the previous section. The laptop in the ground station used the Mission Planner software to communicate and control the drone. The diagram in Figure 4.3 shows how all the parts connect.

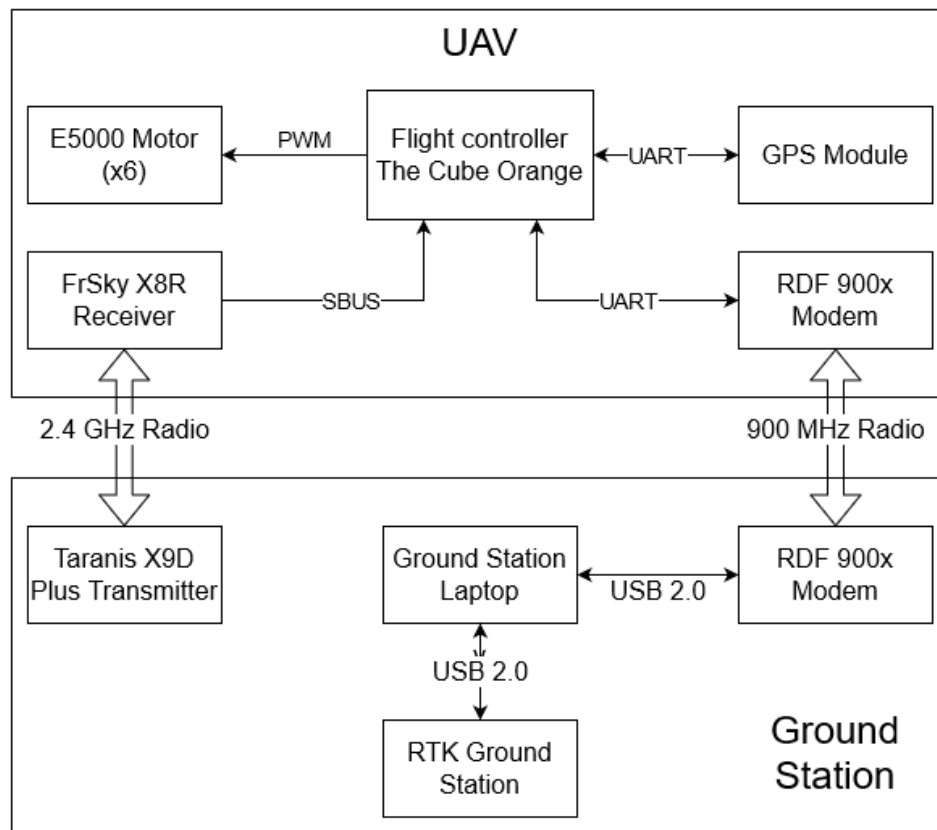


Figure 4.3 Diagram of the electrical component on the UAV and the ground station.

5. CONCLUSION AND FUTURE WORKS

5.1 Conclusion

For the automated leaf-level HSI of soybean plants using a UAV project, a new LeafSpec is developed to work with fragile soybean leaves by shielding the leaf between two sheets of glass. The process of scanning the leaf using LeafSpec is automated by using a motorized rack and pinion mechanism. The new LeafSpec uses a slider-crank mechanism for grasping onto the leaves. The new LeafSpec is also compatible with working as an end-effector of a robotic system such as a 6 DOF robotic arm. Using the high-resolution HS images provided by LeafSpec, it was shown that using the NDVI heatmap for modeling produces better accuracy for N content prediction than the mean NDVI of the leaf. The comparison also shows taking the average of the entire plant or leaf results in the loss of some of the information collected. The correlation between the N content prediction and ground truth has an R^2 value of 0.805 and 0.871 for mean NDVI modeling and NDVI heatmap modeling, respectively. The RMSE of the mean NDVI modeling is 0.338 and 0.276 for NDVI heatmap modeling. Lastly, a UAV designed to carry a 6 DOF robotic arm and LeafSpec is configured and built using open-source hardware and software for easier modification for the later part of the overall project.

5.2 Future Works

Although much work has been done on the LeafSpec and the UAV, there are still improvements to be made. The future work of each part of the project is discussed below.

5.2.1 LeafSpec for Soybean Leaf

Although the current LeafSpec can produce high-quality and high-resolution HS images, there are several areas of improvement to be made to further increase the quality of the images and usability of the device:

1. The mirror size can be shrunk because only a single strip of light needs to be reflected into the camera since the HSC is a line-scanning camera. By reducing the size of the mirror, less unnecessary reflection occurs which can decrease the imaging quality.

2. The overall weight of the LeafSpec can be reduced using acrylonitrile butadiene styrene (ABS) plastic as the material for the case of the device instead of aluminum. The weight reduction can make the LeafSpec more user-friendly with less power consumption required to manipulate it using a robotic system.
3. The communication between the Raspberry Pi and Arduino can be changed to using a robotics operating system (ROS) over UART. ROS provides a robust robot communication protocol that has built-in error correction which increases the reliability of the LeafSpec.

5.2.2 HS images Modeling using Leaf Distribution

The purpose of the current modeling method is to show the non-uniformity within the leaf contains more signals than using a mean value for a leaf. Below are ideas that may further increase the accuracy of the model prediction:

1. In addition to using NDVI, more wavelengths or indexes can be used to improve the accuracy of prediction.
2. A program can be written which tries to find the best combination of wavelengths to predict plant traits.

5.2.3 In-Field UAV for Leaf-Level HS images Collection

The UAV configured and built for this project is still at the early stage of development. Several tasks need to be completed before attaching the robotic arm and LeafSpec on the UAV:

1. The parameters of the proportional-integral-derivative (PID) control for the roll, pitch, and yaw need to be tuned for stable hovering. When using the default parameters, the UAV can drift while hovering due to wind.
2. A new landing skid needs to be designed to absorb the weight of the entire UAV when landing and accommodate the robotic arm and LeafSpec. The current landing skid is designed for agricultural spraying which usually does not have a large landing weight. However, for this project, the landing weight is significantly higher and the optical system in LeafSpec is sensitive to shock and vibration.

REFERENCE

- Chen, Z., Wang, J., Wang, T., Song, Z., Li, Y., Huang, Y., Wang, L., & Jin, J. (2021). Automated in-field leaf-level hyperspectral imaging of corn plants using a Cartesian robotic platform. *Computers and Electronics in Agriculture*, 183, 105996. <https://doi.org/10.1016/j.compag.2021.105996>
- Ge, Y., Bai, G., Stoerger, V., & Schnable, J. C. (2016). Temporal dynamics of maize plant growth, water use, and leaf water content using automated high throughput RGB and hyperspectral imaging. *Computers and Electronics in Agriculture*, 127, 625–632. <https://doi.org/10.1016/j.compag.2016.07.028>
- Godfray, H. C. J., Beddington, J. R., Crute, I. R., Haddad, L., Lawrence, D., Muir, J. F., Pretty, J., Robinson, S., Thomas, S. M., & Toulmin, C. (2010). Food Security: The Challenge of Feeding 9 Billion People. *Science*, 327(5967), 812 LP – 818. <https://doi.org/10.1126/science.1185383>
- Gowen, A. A., O'Donnell, C. P., Cullen, P. J., Downey, G., & Frias, J. M. (2007). Hyperspectral imaging - an emerging process analytical tool for food quality and safety control. *Trends in Food Science and Technology*, 18(12), 590–598. <https://doi.org/10.1016/j.tifs.2007.06.001>
- Hyperspectral Imaging for Thyroid and Salivary Gland Tumor Detection*. (2020). FindLight Blog. <https://www.findlight.net/blog/2020/03/15/hyperspectral-imaging-for-tumor-detection/>
- Kanning, M., Kühling, I., Trautz, D., & Jarmer, T. (2018). High-resolution UAV-based hyperspectral imagery for LAI and chlorophyll estimations from wheat for yield prediction. *Remote Sensing*, 10(12), 2000. <https://doi.org/10.3390/rs10122000>
- Lavado, R. S., Porcelli, C. A., & Alvarez, R. (2001). Nutrient and heavy metal concentration and distribution in corn, soybean and wheat as affected by different tillage systems in the Argentine Pampas. *Soil and Tillage Research*, 62(1–2), 55–60. [https://doi.org/10.1016/S0167-1987\(01\)00216-1](https://doi.org/10.1016/S0167-1987(01)00216-1)
- Li, L., Zhang, Q., & Huang, D. (2014). A Review of Imaging Techniques for Plant Phenotyping. In *Sensors* (Vol. 14, Issue 11). <https://doi.org/10.3390/s141120078>
- Ma, D., Carpenter, N., Amatya, S., Maki, H., Wang, L., Zhang, L., Neeno, S., Tuinstra, M. R., & Jin, J. (2019). Removal of greenhouse microclimate heterogeneity with conveyor system for indoor phenotyping. *Computers and Electronics in Agriculture*, 166, 104979. <https://doi.org/10.1016/j.compag.2019.104979>
- Ma, D., Rehman, T. U., Zhang, L., Maki, H., Tuinstra, M. R., & Jin, J. (2021). Modeling of diurnal changing patterns in airborne crop remote sensing images. *Remote Sensing*, 13(9), 1–19. <https://doi.org/10.3390/rs13091719>

- Masuda, T., & Goldsmith, P. D. (2009). World soybean production: Area harvested, yield, and long-term projections. *International Food and Agribusiness Management Review*, 12(4), 143–162. <https://doi.org/10.22004/ag.econ.92573>
- Mishra, P., Asaari, M. S. M., Herrero-Langreo, A., Lohumi, S., Diezma, B., & Scheunders, P. (2017). Close range hyperspectral imaging of plants: A review. In *Biosystems Engineering* (Vol. 164, pp. 49–67). Academic Press. <https://doi.org/10.1016/j.biosystemseng.2017.09.009>
- Mohd Asaari, M. S., Mishra, P., Mertens, S., Dhondt, S., Inzé, D., Wuyts, N., & Scheunders, P. (2018). Close-range hyperspectral image analysis for the early detection of stress responses in individual plants in a high-throughput phenotyping platform. *ISPRS Journal of Photogrammetry and Remote Sensing*, 138, 121–138. <https://doi.org/10.1016/j.isprsjprs.2018.02.003>
- orthorectification* – *OSSIM*. (n.d.). Retrieved June 9, 2021, from <https://trac.osgeo.org/ossim/wiki/orthorectification>
- Pagano, M. C., & Miransari, M. (2016). The importance of soybean production worldwide. In *Abiotic and Biotic Stresses in Soybean Production*. Elsevier Inc. <https://doi.org/10.1016/B978-0-12-801536-0/00001-3>
- Palmer, C. (2005). *Diffraction Grating Handbook-5th Edition*. THERMO RGL. <http://www.gratinglab.com/http://www.gratinglab.com/library/handbook5/handbook.asp>
- Pölönen, I., Saari, H., Kaivosoja, J., Honkavaara, E., & Pesonen, L. (2013). Hyperspectral imaging based biomass and nitrogen content estimations from light-weight UAV. *Remote Sensing for Agriculture, Ecosystems, and Hydrology XV*, 8887(October), 88870J. <https://doi.org/10.1117/12.2028624>
- Virlet, N., Sabermanesh, K., Sadeghi-Tehran, P., & Hawkesford, M. J. (2017). Field Scanalyzer: An automated robotic field phenotyping platform for detailed crop monitoring. *Functional Plant Biology*, 44(1), 143–153. <https://doi.org/10.1071/FP16163>
- Wang, L., Jin, J., Song, Z., Wang, J., Zhang, L., Rehman, T. U., Ma, D., Carpenter, N. R., & Tuinstra, M. R. (2020). LeafSpec: An accurate and portable hyperspectral corn leaf imager. *Computers and Electronics in Agriculture*, 169. <https://doi.org/10.1016/j.compag.2019.105209>
- Wendel, A., Underwood, J., & Walsh, K. (2018). Maturity estimation of mangoes using hyperspectral imaging from a ground based mobile platform. *Computers and Electronics in Agriculture*, 155, 298–313. <https://doi.org/10.1016/j.compag.2018.10.021>
- Yu, X., Lu, H., & Liu, Q. (2018). Deep-learning-based regression model and hyperspectral imaging for rapid detection of nitrogen concentration in oilseed rape (*Brassica napus* L.) leaf. *Chemometrics and Intelligent Laboratory Systems*, 172, 188–193. <https://doi.org/10.1016/j.chemolab.2017.12.010>